Water Air Soil Pollut (2019) 230: 70
https://doi.org/10.1007/s11270-019-4125-x

# Production of Biochar from Food Waste and its Application for Phenol Removal from Aqueous Solution

**Chang-Gu Lee · Seung-Hee Hong · Seong-Gu Hong · Jae-Woo Choi · Seong-Jik Park**

Received: 31 October 2018 / Accepted: 15 February 2019 / Published online: 26 February 2019


**Abstract** Deriving biochar from biowaste facilitates its reuse and application for environmental protection. This study addresses the adsorption of phenol onto food waste–based biochar (FWC). Phenol adsorption on FWC was affected by pyrolysis temperature, and the highest adsorption capacity was found at a temperature of 700 °C (FWC700). The characteristics of the biochar including morphology, surface area, functional groups, and elemental composition were analyzed. Additional batch experiments were performed to evaluate the phenol adsorption on FWC700 under various experimental conditions such as contact time, initial concentration, reaction temperature, solution pH, adsorbent dose, and presence of competing ions. The adsorption capacity of phenol decreased gradually from 9.79 ± 0.04 to 8.86 ± 0.06 mg/g between solution pH of 3 and 11. Copper sulfate showed the greatest interference on phenol adsorption to FWC in aqueous solution. Phenol removal at different contact times followed pseudo-second-order kinetics, and the Langmuir isotherm model provided the best fit of the equilibrium data with a maximum adsorption capacity of 14.61 ± 1.38 mg/g. Adsorption of phenol increased with increasing temperature from 15 to 35 °C, and thermodynamic analysis indicated an endothermic and spontaneous nature of the adsorption process. Biochar derived from food waste can be used as bio-adsorbent for the removal of phenol from aqueous solution.

**Keywords** Food waste · Biochar · Pyrolysis temperature · Phenol removal · Adsorption

C.-G. Lee
Department of Environmental and Safety Engineering, Ajou University, Suwon, South Korea

S.-H. Hong · S.-G. Hong · S.-J. Park (✉)
Department of Bioresources and Rural System Engineering, Hankyong National University, Anseong, South Korea
e-mail: parkseongjik@hknu.ac.kr

J.-W. Choi
Center for Water Resource Cycle Research, Korea Institute of Science and Technology, Seoul, South Korea

## 1 Introduction

Phenolic compounds, considered priority pollutants due to their high toxicity and potential accumulation in the environment, are present in the effluents of various industries such as petroleum refining, leather and textile manufacturing, wood processing, pharmaceuticals, and oil manufacturing industries with high concentration up to even several thousands of mg/L (Polat et al. 2006; Calace et al. 2002; Lin and Juang 2009). Discharge of these compounds without treatment leads to serious threats to human health with acute and chronic symptoms. Phenolic compounds irritate skin, eyes, and mucous membranes in humans. Anorexia, weight loss, diarrhea, vertigo, salivation, and dark coloration of the urine have been reported in cases of chronic exposure, and severe cases lead to coma and respiratory arrest (Substances and Registry 1998; Villegas et al. 2016). Therefore, the US Environmental Protection Agency (EPA) and the World Health Organization (WHO) set

a limit for phenol of less than 1 μg/L in surface water (Villegas et al. 2016; Mukherjee et al. 2007).

Various physical, chemical, and biological treatment techniques have been developed for the removal of phenol from aqueous solution, including membrane filtration (Zagklis et al. 2015), reverse and forward osmosis (Cui et al. 2016), ion exchange (Víctor-Ortega et al. 2016), electrochemical oxidation (Garcia-Segura et al. 2018), photo-catalytic degradation (Lee et al. 2018), aerobic and anaerobic biodegradation (Papaevangelou et al. 2016), and adsorption (Liu et al. 2010; Jain et al. 2004). Among these, adsorption is the most effective and widely used technology for removal of phenol because it can effectively remove various contaminants and is convenient in design and operation. Therefore, the USEPA recommends adsorption on activated carbon as a best available technique for organic contaminants including phenolic compounds, and activated carbon has been used in practical research due to its high adsorption capacity and mechanical stability (Mukherjee et al. 2007; Hamdaoui and Naffrechoux 2007). However, due to the relatively high cost of activated carbon, many researchers have been interested in developing alternative low-cost carbonaceous adsorbents using natural and abundant raw materials such as switchgrass, animal manure, and sewage sludge (Regmi et al. 2012; Idrees et al. 2018; Julcour Lebigue et al. 2010). Shin (2017) studied the adsorption characteristics of phenol and heavy metals on biochar from *Hizikia fusiformis*, and Peng et al. (2016) investigated the impacts of pH, inorganic fractions, and dissolved organic carbon on pentachlorophenol adsorption on reed biochar. Zheng et al. (2017) studied the adsorption of p-nitrophenols on microalgal biochar. Jung et al. (2013) examined the thermal process to produce biochar under the oxygen-limited condition, which allowed higher surface area and consequently better adsorption of endocrine disrupting compounds. Han et al. (2013) also studied the heavy metal and phenol adsorptive properties of biochar from pyrolyzed switchgrass and woody biomass.

Recently, abuse of food has caused the generation of excessive amounts of food waste (FW), which has become a serious concern in many countries. FW generally contains high moisture and protein-rich organic matter, which can easily become rotten in ambient conditions and cause odor and leachate problems. This makes collection and transportation difficult and adversely affects the environment if the FW is landfilled (Lee et al. 2009; Kim and Kim 2010). In South Korea, about 13,000 tons of FW is generated each day, which corresponds to approximately 27% of the total solid waste. Landfilling of FW has been banned in South Korea since 2005. More than 90% of the FW is recycled as feedstock for animals, fertilizer, and other uses, including biogas generation in anaerobic digesters, with proportions of 41.6%, 32.0%, and 16.8%, respectively, even though use for animal feed has been prohibited in the EU (MOE 2017; Kim and Kim 2010). As an abundant raw material, FW can also be used to produce biochar via thermochemical conversion. Gupta et al. (2018) prepared biochar from food and wood wastes as an additive for carbon sequestration in cement mortar, and Rago et al. (2018) assessed the potential of biochar production from food wastes as a biofuel. Only the above two studies have been reported using biochar derived from food waste, and as far as we know, food waste–based biochar has never been applied for the removal of contaminants from aqueous solutions.

Therefore, in this study, local food waste–based biochar (FWC) was prepared and applied to investigate its ability for phenol removal from aqueous solution. The FWC was synthesized at various temperatures and characterized via scanning electron microscopy, BET surface area, Fourier-transform infrared spectroscopy, and elemental analysis. The phenol adsorption ability of FWC was evaluated under various experimental conditions, such as contact time, initial concentration, reaction temperature, solution pH, adsorbent dose, and presence of competing ions. Kinetic, isotherm, and thermodynamic adsorption model analyses were also conducted to understand the phenol adsorption characteristics of the FWC.

## 2 Materials and Methods

### 2.1 Preparation of Adsorbent

The FW used in this study was obtained from a food waste treatment plant located in Seoul, South Korea. The pre-treatment process for the FW is described elsewhere (Kim et al. 2018a). Briefly, the water contained in the FW was squeezed out by a screw press, and the material was dried further using a steam boiler at 150 °C. After grinding the dried FW, foreign substances were removed sequentially by a magnetic separator and a trommel separator.

To obtain biochar from the FW, the parent materials were carbonized at various temperatures (300, 500, 700, and 900 °C) under a flow of nitrogen. Then, the FW–derived biochar was treated with 0.1 N $HNO_3$ at 25 °C for 1 week. After that, the FWC was rinsed with deionized water and dried at 60 °C for 12 h using a vacuum oven. The dried FWC was stored in a desiccator for further use. Commercial activated carbon for comparative study of adsorption capacity was supplied by a local company, Kaya Carbon Company. The activated carbon with a grain size of 1.18–2.36 mm was used without further cleaning.

### 2.2 Characterization

A field emission scanning electron microscope (FESEM, S-4700, Hitachi, Japan) was used to obtain microscopic images of the biochar. Brunauer, Emmet, and Teller (BET) surface area was measured using an Autosorb-iQ 2ST/MP analyzer (Quantachrome, USA) at 77.35 K. Fourier-transform infrared spectroscopy (FTIR) was performed on a Nicolet iS10 spectrometer (Thermo Scientific, USA). The contents of C, H, N, and S were measured using a 2400 Series II CHNS/O elemental analyzer (PerkinElmer, USA). To determine the pH, biochar and deionized water were mixed at a ratio of 1:5, the mixture was stirred for 1 h, and then pH was measured using a pH meter (Seven-Multi S40, Mettler Toledo, Switzerland).

### 2.3 Adsorption Study

Adsorption experiments were conducted in triplicate under batch conditions to evaluate the adsorbent ability of FWC for phenol. Phenol standard solution (1000 μg/mL in water) was purchased from AccuStandard® and diluted with deionized water for the experiments. All experiments were carried out in a 50 mL conical tube and shaken using a shaking incubator (SHAK116, Vison Scientific Co., Korea) at 100 rpm. First, the influence of the activation temperature of the FWC on phenol removal was evaluated. A mass of 0.1 g of each adsorbent (5 g/L) was added to a conical tube containing 20 mL of 10 mg/L phenol solution. After 24 h of reaction, the phenol solution was separated from the adsorbent using filter paper (no. 1822-047, Whatman, USA), and the residual phenol concentration was analyzed via standard methods of UV/visible spectroscopy at 510 nm using a spectrophotometer (Optizen POP QX, Mecasys, Korea).

Other adsorption experiments were carried out using the FWC activated at 700 °C (FWC700). Contact time experiments were conducted during 15, 30, 60, 120, 180, 360, 720, and 1440 min (initial phenol concentrations of 10 and 50 mg/L, biochar dose of 3.33 g/L), and reaction temperature experiments were carried out at 15, 25, and 35 °C during the same time intervals (initial phenol concentration of 50 mg/L, biochar dose of 3.33 g/L). Initial concentration tests were performed at phenol concentrations of 10–200 mg/L (biochar dose of 3.33 g/L, contact time of 24 h). To assess adsorption performance in environmental relevant water, a synthetic water was prepared by dissolving the following reagent grade chemicals to deionized water: 252 mg/L $NaHCO_3$, 147 mg/L $CaCl_2$, 124 mg/L $MgSO_4 \cdot 7H_2O$, 95 mg/L $Na_2SiO_3 \cdot 9H_2O$, 12 mg/L $NaNO_3$, 2.2 mg/L NaF, 0.18 mg/L $NaH_2PO_4 \cdot H_2O$. For the pH test, 0.1 M HCl and 0.1 M NaOH were used to adjust the pH of the solution to 3, 5, 7, 9, and 11 (initial phenol concentration of 50 mg/L, biochar dose of 3.33 g/L, contact time of 24 h). Adsorbent dose experiments were carried out using 0.1, 0.2, 0.3, 0.4, and 0.5 g of biochar with 30 mL of 50 mg/L phenol solution for 24 h. The effect of competing ions on phenol adsorption was investigated in the presence of 1 and 10 mM $NaHCO_3$, $NaNO_3$, $Na_2HPO_4$, $CaCO_3$, $CuSO_4$, and $MgSO_4$ solutions, respectively (initial phenol of concentration 50 mg/L, biochar dose of 3.33 g/L, contact time of 24 h). Bisphenol A (BPA, ≥ 99% purity) is purchased from Sigma Aldrich and diluted with deionized water for the experiments. BPA concentration was analyzed using a high-performance liquid chromatograph (LC-20AT, Shimadzu, Japan) equipped with a C-18 column (dC18 Column, Atlantis) and an UV−vis detector (SPD-M20A, Shimadzu, Japan) at the mobile phase (60% acetonitrile and 40% water) flow rate of 1.0 mL/min and injection volume of 20 μL.

## 3 Results and Discussion

### 3.1 Activation with Different Temperature

Food waste–based biochar (FWC) was pyrolyzed over a wide range of temperatures to determine effective heat treatment conditions for phenol removal. Phenol adsorption on FWC increased gradually with pyrolysis temperature up to 700 °C and decreased slightly at 900 °C (Fig. 1). The plateau formation by pyrolysis temperature

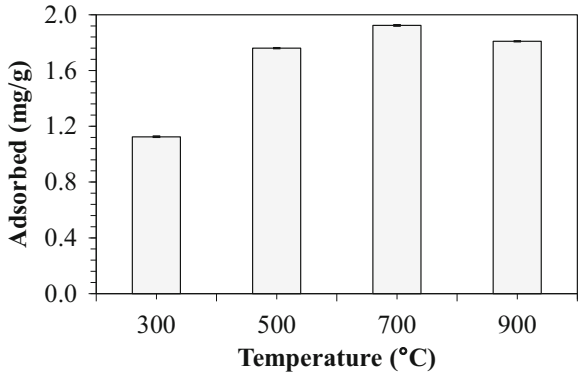


**Fig. 1** Effect of activation temperature of food waste-based biochar on phenol removal (initial phenol concentration of 10 mg/L, biochar dose of 5 g/L, contact time of 24 h)

was related with three main steps of biomass pyrolysis: (1st step) biomass → water + unreacted residue; (2nd step) unreacted residue → $(\text{volatile} + \text{gases})_1 + (\text{char})_1$; (3rd step) $(\text{char})_1 \rightarrow (\text{volatile} + \text{gases})_2 + (\text{char})_2$ (Demirbas 2004; Li et al. 2017). Moisture and some volatile were removed in the initial step, whereas primary biochar occurred in the second step. Biochars produced at moderate temperature (500–700 °C) during the primary carbonization process (< 700 °C) have been reported to have higher adsorption capacity for organic contaminants than biochars generated at relatively low temperature (300 °C) (Vithanage et al. 2016; Ahmad et al. 2012; Chen and Chen 2009) because the carbonization degree and aromaticity of biochar become higher by increasing temperature. In the last step, however, chemical rearrangement occurs due to additional heat treatment; thus, collapse of the structure blocks pores and the reactivity of the biochar is reduced (Li et al. 2017; Demirbas 2004). Based on the phenol adsorption results, the FWC pyrolyzed at 700 °C (FWC700) was used for further adsorption tests and characterizations.

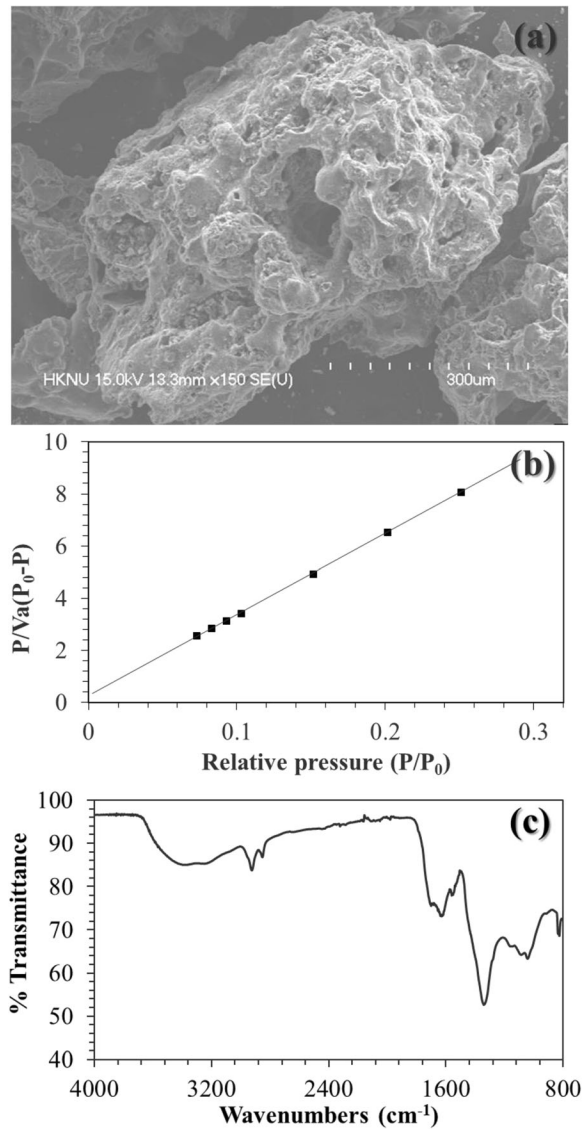


**Fig. 2** Characteristics of FWC700. **a** SEM image. **b** BET fitting. **c** FTIR spectrum

### 3.2 Characteristics of Biochar

The scanning electron microscopy (SEM) image of FWC700 exhibited the development of a void-porous structure on the surface (Fig. 2a). The specific surface area of the FWC700 calculated via BET fitting (Fig. 2b) was 110.98 $m^2/g$, which is within the common range of biochar derived from various biowastes, such as tea waste (342.22 $m^2/g$) (Vithanage et al. 2016), rice straw (50.62 $m^2/g$) (Li et al. 2017), manure waste (60.0 $m^2/g$) (Idrees et al. 2018), and sewage sludge (125 $m^2/g$) (Julcour Lebigue et al. 2010). The pore structure and large surface area were generated through the evaporation of volatile components (2nd step of the pyrolysis process), which provides enlarged adsorption sites for contaminant.

Surface functional groups of FWC700 were probed via FTIR analysis (Fig. 2c). The broad peak at 3368 $cm^{-1}$ in the spectrum represents the presence of the O−H stretching vibration of alcohols, phenols, and carboxylic acid groups (Vithanage et al. 2016; Dong et al. 2013). The bands at 2926 $cm^{-1}$ and 2854 $cm^{-1}$ were assigned to the aliphatic $-CH_2$ stretching vibration, and the peak at 1629 $cm^{-1}$ represents C=O and

C=C stretching in aromatic rings (Ahmad et al. 2012; Yang et al. 2018). The peaks at 1340 $cm^{-1}$ and 1041 $cm^{-1}$ correspond to the stretching vibration of methyl C−H and the oxygenated functional group of O−H, respectively (Baoliang Chen et al. 2008). The peak at 824 $cm^{-1}$ of the FWC700 was assigned to aromatic C−H groups, which indicates the condensation of the biochar structure (Dong et al. 2013; Yang et al. 2018).

Elemental analysis of the FWC700 was conducted, and the results are presented in Table 1. The C content of the sample was 57.11 wt%, and the H and N contents were 2.27 wt% and 5.42 wt%, respectively. The S content was negligibly low. The aromaticity of biochar is generally evaluated by the molar ratio of H/C, for which a value lower than 0.3 indicates a highly condensed aromatic ring system and a value greater than 0.8 means a non-condensed structure (Cely et al. 2014). As examples, the H/C value of granular sludge biochar was 0.23 (Kim et al. 2018b) and that of biochar derived from rice straw was 0.88 (Li et al. 2017). The H/C molar ratio of FWC700 was 0.52, which is between these common values of biochar. The pH of FWC700 was 6.40 due to the sufficient rinsing process after modification.

## 3.3 Phenol Adsorption Experiments

### *3.3.1 Effect of Contact Time*

The phenol adsorption by FWC700 as a function of contact time is provided in Fig. 3. At the low phenol concentration of 10 mg/L, adsorption was completed within 30 min and equilibrium was reached because no additional phenol was present in the aqueous solution. The adsorbed phenol did not become detached until 24 h of contact time. Uptake of phenol at the high concentration (50 mg/L) occurred rapidly during the initial period of reaction time and reached 10.91 ± 0.13 mg/g at 3 h. The rapid adsorption was due to the large number of active sites remaining on the adsorbent surface at this stage (Idrees et al. 2018; Vikrant et al. 2018). Phenol uptake on FWC700 gradually increased further to 12.63 ± 0.16 mg/g at 24 h.

**Table 1** Basic properties of the food waste–based biochar (FWC700)

| C (wt%) | H (wt%) | N (wt%) | S (wt%) | pH (−) | Surface area ($m^2$/g) |
|---|---|---|---|---|---|
| 57.11 | 2.27 | 5.42 | nd | 6.40 | 110.98 |

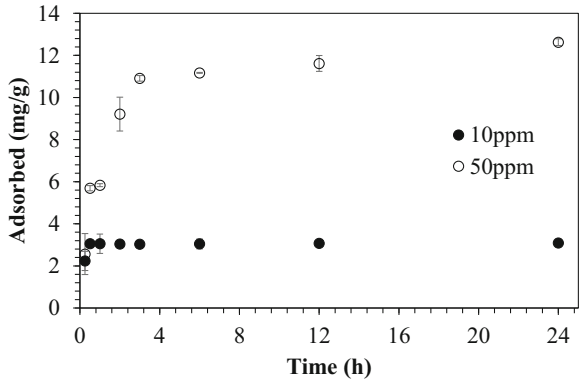


**Fig. 3** Effect of contact time on phenol removal with FWC700 (initial phenol concentrations of 10 and 50 mg/L, biochar dose of 3.33 g/L)

### *3.3.2 Effect of Initial Concentration*

The effect of initial concentration on adsorption of phenol was evaluated, as shown in Fig. 4. The adsorption

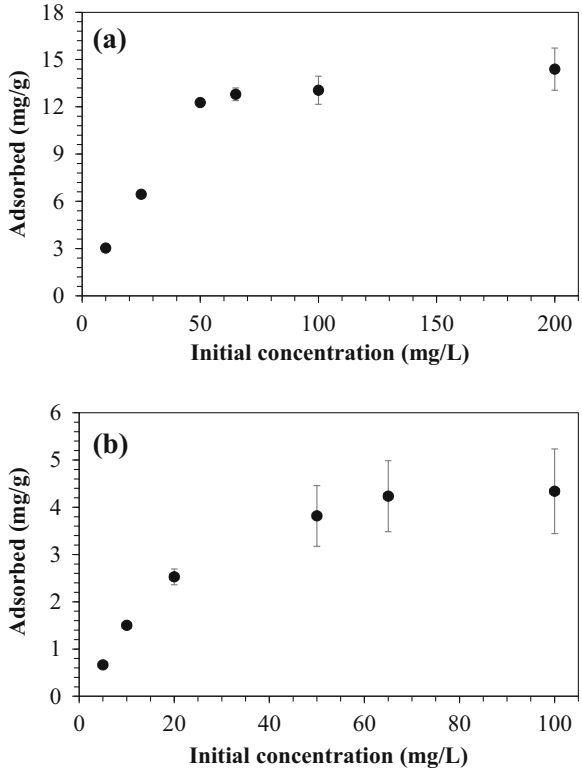


**Fig. 4** Effect of initial phenol concentration on phenol removal in **a** deionized water and in **b** synthetic model water (biochar dose of 3.33 g/L, contact time of 24 h)

amount increased with increasing initial phenol concentration from 10 to 200 mg/L because the driving force between adsorbate and adsorbent increases as the initial concentration increases (Idrees et al. 2018; Lee et al. 2016). At the lowest concentration of 10 mg/L, phenol was adsorbed completely to the adsorbent dose of 3.33 g/L and the adsorption amount of phenol was calculated as 3.00 ± 0.01 mg/g. The adsorption amount increased to 12.80 ± 0.40 mg/g at the initial phenol concentration of 65 mg/L and increased further to 14.39 ± 1.34 mg/g at the highest concentration of 200 mg/L. The removal ratio of phenol decreased from 86.01 to 23.99% with increasing concentration from 25 to 200 mg/L. In addition, phenol adsorption experiments were also carried out in synthetic water to assess the performance of EFC700 in environmental relevant water. The adsorption of phenol increased with increasing initial concentration and reached to 4.34 ± 0.90 mg/g with the initial phenol concentration of 100 mg/L. This value was one-third of the result obtained from using deionized water because coexisting ions in synthetic water can interfere with the adsorption of phenol onto FWC700.

### 3.3.3 Effect of Reaction Temperature

The effect of reaction temperature on the adsorption of phenol by FWC700 was investigated at 15 °C, 25 °C, and 35 °C, and the adsorption amounts of FWC700 according to reaction time are shown in Fig. 5. The results indicated that phenol adsorption was increased by higher temperature, and the adsorption amount reached 9.74 ± 0.62 mg/g at 15 °C and 13.49 ± 0.40 mg/g at 35 °C after 24 h of reaction. Therefore, the phenol adsorption reaction onto FWC700 was endothermic in nature, which was ascribed to the increase of diffusion of adsorbate molecules across the internal pores of the adsorbent with increasing temperature. Similar endothermic reactions were observed for naphthalene and 1,3-dinitrobenzene adsorption on biomass-derived biochars (Chen et al. 2012).

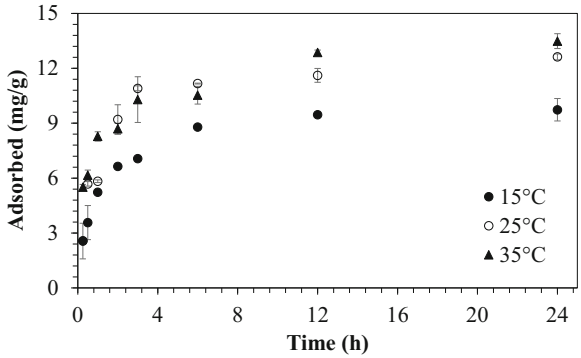


**Fig. 5** Effect of reaction temperature on phenol adsorption (initial phenol concentration of 50 mg/L, biochar dose of 3.33 g/L)

### 3.3.4 Effect of Solution pH

The adsorption of phenolic compounds from aqueous solution onto carbonaceous adsorbents is generally dependent on the solution pH, which affects the degree of ionization and speciation of the adsorbate (Zheng et al. 2017; Shin 2017). Phenol removal by FWC700 as a function of solution pH is illustrated in Fig. 6. The results showed that phenol adsorption decreased gradually from 9.79 ± 0.04 to 8.86 ± 0.06 mg/g as the solution pH increased from 3 to 10. This reduction was attributed to the continuous ionization of the phenol molecules and the increase in electrostatic repulsions with increase of pH. Similar behaviors have been reported for the adsorption of phenol onto biochar from *H. fusiformis* and rice husk ash (Shin 2017; Mahvi et al. 2004), respectively.

### 3.3.5 Effect of Adsorbent Dose

The effect of adsorbent dose on the removal of phenol by FWC700 was studied by varying the amount of adsorbent from 0.1g (3.33 g/L) to 0.5 g (16.67 g/L). The results of the adsorption amount and removal ratio of 50 mg/L phenol in 30 mL of solution are shown in

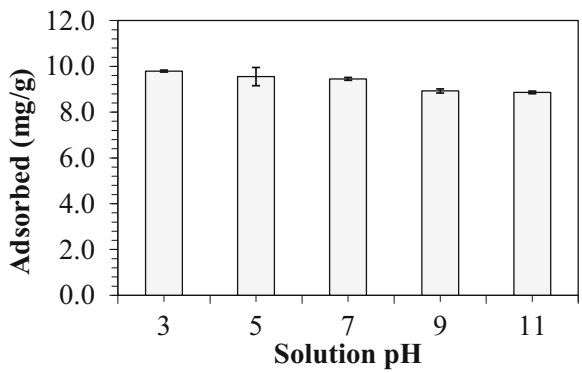


**Fig. 6** Effect of solution pH on phenol adsorption (initial phenol concentration of 50 mg/L, biochar dose of 3.33 g/L, contact time of 24 h)

Fig. 7. The adsorption amount of phenol decreased with increasing adsorbent dose. At 3.33 g/L, the adsorption amount was 9.91 ± 0.52 mg/g, but the amount decreased sharply to 5.02 ± 0.06 mg/g at 6.67 g/L. The adsorption amount decreased to 3.79 ± 0.04 mg/g at 10 g/L of adsorbent dose and decreased further to 2.40 ± 0.00 mg/g at 16.67 g/L. The removal ratio increased with increasing adsorbent dose. The removal ratio was 66.10% at the adsorbent dose of 3.33 g/L but increased to 75.34% at 10 g/L. The ratio exceeded 80% at the adsorbent dose of 16.67 g/L.

### 3.3.6 Presence of Competing Ions

The effect of competing ions on phenol adsorption was evaluated with $NaHCO_3$, $NaNO_3$, $Na_2HPO_4$, $CaCO_3$, $CuSO_4$, and $MgSO_4$ salts, and the adsorption amount of phenol decreased with increasing molar concentration of each salt from 0 to 10 mM (Fig. 8). The adsorption of phenol was decreased by 1 mM salts in the order of $NaNO_3$, $Na_2HPO_4$, $NaHCO_3$, $MgSO_4$, $CaCO_3$, and $CuSO_4$, but it was decreased in the order of $NaNO_3$, $NaHCO_3$, $MgSO_4$, $CaCO_3$, $Na_2HPO_4$, and $CuSO_4$ at 10 mM. Industrial wastewaters containing phenol usually also include a variety of interfering ions that can affect the adsorption of phenol to carbon materials (T. Y. Kim et al. 2010; Lazo-Cannata et al. 2011; Arafat et al. 1999). Adsorption can be enhanced at low salt concentrations by charge neutralization and the salts-out effect, but it can be diminished at high concentrations due to the formation of water clusters on surface functional groups such as carboxylic acids. The reduction of phenol adsorption with increasing salt concentration was well explained by the latter water adsorption effect. At

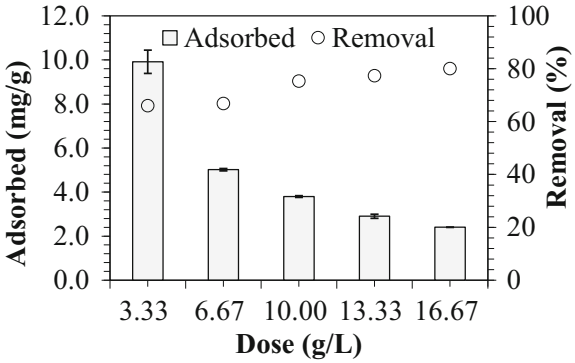


**Fig. 7** Effect of biochar dose on phenol adsorption and removal rate (initial phenol concentration of 50 mg/L, contact time of 24 h)

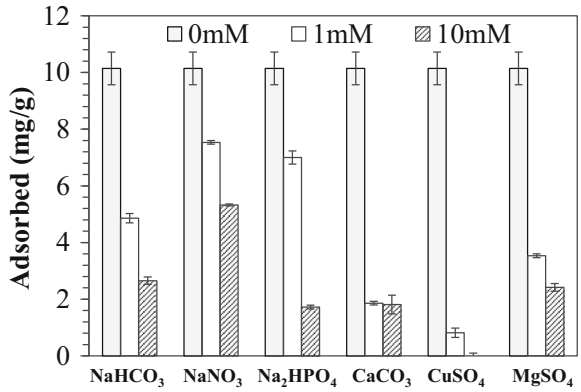


**Fig. 8** Effect of competing ions on phenol adsorption (initial phenol concentration of 50 mg/L, biochar dose of 3.33 g/L, contact time of 24 h)

both the 1 and 10 mM salt concentrations, $CuSO_4$ hindered phenol adsorption the most in our experimental condition. This occurred because both copper and sulfate ions can compete with the adsorption of phenol on carbon materials (Honfi et al. 2016; Varghese et al. 2004).

### 3.3.7 Bisphenol A Adsorption Test

Bisphenol A (BPA) is a commonly encountered endocrine disrupting chemicals and has been studied by several researchers as a representative harmful phenolic compound in aqueous solution (Javed et al. 2018; Zhang et al. 2018). Here, the adsorption of BPA on FWC700 was also evaluated for comparison with phenol, since both compounds have different properties such as molecular weight, solubility, and partition coefficient (Ou et al. 2016; Xie et al. 2012). As shown in Fig. 9, the adsorption amount increased with increasing initial BPA concentration. The adsorption amount increased to

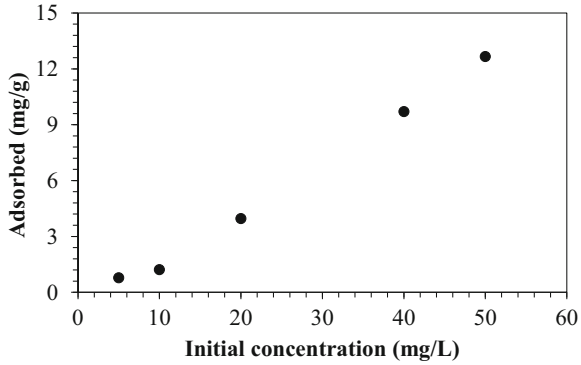


**Fig. 9** Bisphenol adsorption in FWC700 according to initial concentration (biochar dose of 3.33 g/L, contact time of 24 h)

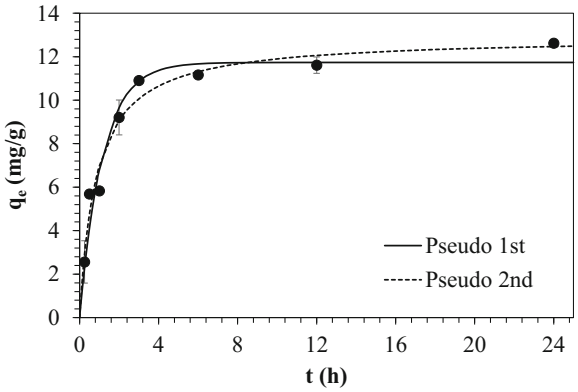


**Fig. 10** Kinetics of phenol adsorption on FWC700 as fitted by pseudo-first-order and pseudo-second-order models. Model parameters are provided in Table 2

12.67 ± 0.01 mg/g at the initial BPA concentration of 50 mg/L, which was slightly higher than phenol (12.27 ± 0.14 mg/g) under the same conditions. Due to the low solubility of BPA, it was incomparable at higher concentrations.

## 3.4 Adsorption Model Study

### *3.4.1 Kinetic Adsorption Models*

The adsorption data provided in Fig. 3 as a function of contact time with 50 mg/L initial phenol concentration were analyzed to determine the kinetic model parameters using pseudo-first-order (Eq. (1)) and pseudo-second-order (Eq. (2)) kinetic models:

$$q_t = q_e\left(1-e^{-k_1 t}\right) \tag{1}$$

$$q_t = \frac{k_2 q_e^2 t}{1 + k_2 q_e t} \tag{2}$$

where $q_t$ and $q_e$ are the adsorbed amount of phenol at time $t$ and equilibrium time and $k_1$ and $k_2$ are the adsorption rate constants of each model, respectively. Based on the model fittings and the parameters provided in Fig. 10 and Table 2, both kinetic models could describe the adsorption data with a high coefficient of determination ($R^2$). The pseudo-second-order model had the optimal fitting ($R^2 = 0.964$, sum of squared errors (SSE) = 3.284), indicating that chemisorption was involved in the phenol adsorption by FWC700. Similar kinetic adsorption properties of phenolic compounds have been reported for several biochars derived from paper sludge/wheat husk, *Hizikia fusiformis*, and microalgae (Shin 2017; Zheng et al. 2017; Kalderis et al. 2017).

### *3.4.2 Adsorption Isotherms*

Nonlinear forms of the Freundlich (Eq. (3)) and Langmuir (Eq. (4)) isotherm models were employed to analyze the adsorption data as a function of initial phenol concentration, as provided in Fig. 4:

$$q_e = K_F C_e^{1/n} \tag{3}$$

$$q_e = \frac{Q_m K_L C_e}{1 + K_L C_e} \tag{4}$$

where $C_e$ is the equilibrium concentration of phenol in the aqueous solution, $K_F$ and $1/n$ are the Freundlich constant related to the adsorption capacity and the adsorption intensity, and $Q_m$ and $K_L$ are the maximum adsorption capacity of biochar and the Langmuir constant related to the affinity of the binding site, respectively. The model fitting is presented in Fig. 11 and the model parameters are provided in Table 3. The higher $R^2$ and lower SSE of the Langmuir model indicated that it was suitable for describing the equilibrium data, suggesting that phenol adsorption onto FWC700 occurred by a homogeneous monolayer adsorption process. The

**Table 2** Kinetic parameters obtained from the pseudo-first-order and pseudo-second-order kinetics models

| Pseudo-first-order model | | | | Pseudo-second-order model | | | |
|---|---|---|---|---|---|---|---|
| $k_1$ (/h) | $q_e$ (mg/g) | $R^2$ (−) | SSE† (−) | $k_2$ (L/mg) | $q_e$ (g/mg/h) | $R^2$ (−) | SSE† (−) |
| 0.864 ± 0.132 | 11.736 ± 0.489 | 0.953 | 4.718 | 0.091 ± 0.019 | 12.914 ± 0.530 | 0.964 | 3.284 |

† SSE: Sum of squared errors

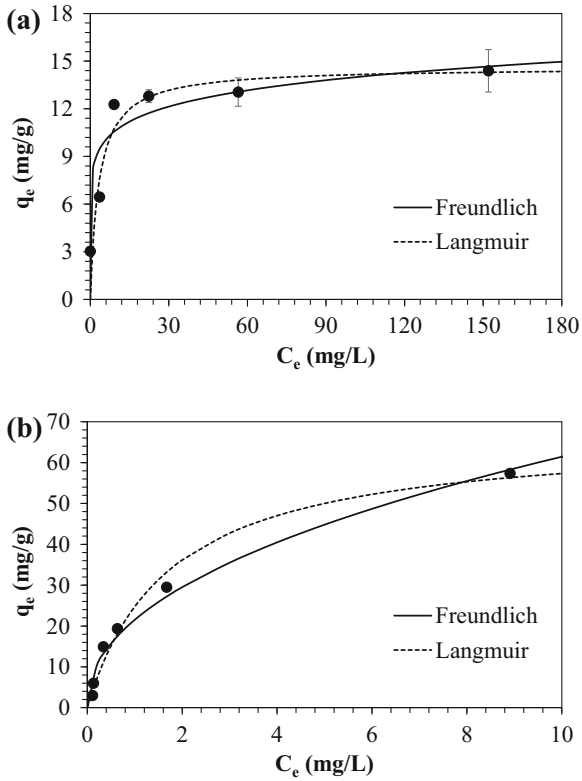


**Fig. 11** Equilibrium model analyses with the Freundlich and Langmuir isotherms. **a** FWC700. **b** commercial activated carbon. Model parameters are provided in Table 3

dimensionless separation factor ($R_L$) of the Langmuir-type adsorption process is defined as follows:

$$R_L = \frac{1}{1 + K_L C_0} \tag{5}$$

where $C_0$ is the initial phenol concentration in the solution. The $R_L$ values calculated from the various initial phenol concentrations (10–200 mg/L) were in the range of 0.016 to 0.248. Values between 0 and 1 indicate a favorable adsorption nature of phenol onto biochar (Bekkouche et al. 2012; Zhou et al. 2018). The Langmuir maximum adsorption capacity ($Q_m$) of phenol onto FWC700 was 14.61 ± 1.38 mg/g, which corresponds to the lower part of the general range of reported phenol adsorption values for biochars of 14.04 mg/g to 83.88 mg/g (Shin 2017; Zhou et al. 2018; Karakoyun et al. 2011; Liu and Zhang 2011). Commercial activated carbon, most widely used adsorbent for the removal of organic contaminants, was also compared with FWC700 under the same experimental condition, and Langmuir maximum adsorption capacity of the activated carbon for phenol was 67.19 ± 4.90 mg/g. Thus, further studies are needed to improve the adsorption capacity of food waste–derived biochar.

### 3.4.3 Adsorption Thermodynamics

The experimental data as a function of reaction temperature presented in Fig. 5 were used to obtain thermodynamic adsorption parameters of phenol on FWC700. Gibbs free energy ($\Delta G^0$), enthalpy ($\Delta H^0$), and entropy ($\Delta S^0$) were determined by the following equations:

$$K_e = \frac{aq_e}{C_e} \tag{6}$$

$$ln(K_e) = \frac{\Delta S^0}{R} - \frac{\Delta H^0}{RT} \tag{7}$$

$$\Delta G^0 = \Delta H^0 - T\Delta S^0 \tag{8}$$

where $K_e$ and $a$ are the dimensionless distribution coefficient and adsorbent dose (g/L), respectively, $R$ is the universal gas constant (= 8.314 J/mol/K), and $T$ is the absolute temperature of solution. A plot of $ln(K_e)$ versus $1/T$ using Eq. (7) is shown in Fig. 12, and the thermodynamic parameters calculated from Eq. (8) are presented in Table 4. The positive enthalpy ($\Delta H^0$) value represents an endothermic nature of phenol adsorption to

**Table 3** Equilibrium adsorption parameters obtained from Freundlich and Langmuir isotherms: (a) FWC700, (b) commercial activated carbon

| Type | Freundlich isotherm | | | | Langmuir isotherm | | | |
|---|---|---|---|---|---|---|---|---|
| | $K_F$ (L/g) | $1/n$ (−) | $R^2$ (−) | SSE (−) | $K_L$ (L/mg) | $Q_m$ (mg/g) | $R^2$ (−) | SSE (−) |
| (a) | 8.16 ± 1.25 | 0.12 ± 0.04 | 0.865 | 13.943 | 0.30 ± 0.16 | 14.61 ± 1.38 | 0.937 | 13.344 |
| (b) | 21.52 ± 1.70 | 0.46 ± 0.04 | 0.979 | 44.004 | 0.58 ± 0.11 | 67.19 ± 4.90 | 0.984 | 33.706 |

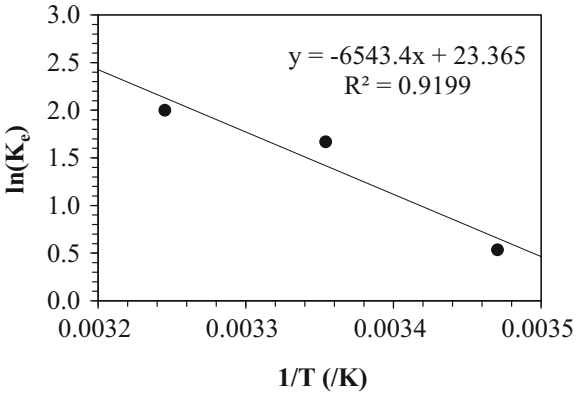


**Fig. 12** Thermodynamic analysis of phenol adsorption on FWC700. Thermodynamic parameters are provided in Table 4

FWC700, which is consistent with the result of the reaction temperature experiment. Additionally, the $\Delta H^0$ value can be used to distinguish between physical adsorption (< 25 kJ/mol) and chemisorption (> 40 kJ/mol) processes (Vithanage et al. 2016; Liu et al. 2015; Polat et al. 2006). The calculated enthalpy ($\Delta H^0$) value for FWC700 was 54.402 kJ/mol, which indicates that the adsorption of phenol was close to chemisorption, agreeing with the result of the pseudo-second-order kinetic adsorption model. The positive entropy ($\Delta S^0$) value indicates increased randomness at the interface between the solid and the solution during the adsorption process. The negative Gibbs free energy ($\Delta G^0$) values in the experiment conditions suggest a spontaneous nature of phenol adsorption to biochar. This endothermic and spontaneous thermodynamic adsorption nature of phenolic compounds was also found for adsorption onto magnetic biochar (Zhou et al. 2018) and paper sludge/wheat husk biochar (Kalderis et al. 2017).

## 4 Conclusion

Food waste–based biochars were successfully synthesized under various pyrolysis temperatures. The biochar synthesized at 700 °C (FWC700) had a high specific surface area with a void-porous structure on the surface and the highest phenol adsorption capacity. The adsorption capacity of phenol decreased with increasing solution pH between 3 and 11 and was affected by the presence of competing ions such as those from copper sulfate. A homogeneous and favorable adsorption nature of phenol through the FWC surface with cooperative chemisorption characteristics was found. Thermodynamic parameters suggested endothermic and spontaneous adsorption of phenol to biochar. Therefore, biochar derived from food wastes is expected to be useful as an alternative low-cost carbonaceous adsorbent for water treatment processes.

**Table 4** Thermodynamic parameters of phenol adsorption on food waste–based biochar (FWC700)

| Temperature (°C) | $\Delta H^0$ (kJ/mol) | $\Delta S^0$ (J/K mol) | $\Delta G^0$ (kJ/mol) |
|---|---|---|---|
| 15 | 54.402 | 194.257 | − 1.573 |
| 25 | | | − 3.516 |
| 35 | | | − 5.458 |

**Funding Information** This research was supported by the New Faculty Research Fund of Ajou University and the National Research Foundation (NRF) of Korea (NRF-2018R1C1B5044937).

**Compliance with Ethical Standards**

**Conflict of Interest** The authors declare that they have no conflict of interest.



## References

Ahmad, M., Lee, S. S., Dou, X., Mohan, D., Sung, J. K., Yang, J. E., et al. (2012). Effects of pyrolysis temperature on soybean stover- and peanut shell-derived biochar properties and TCE adsorption in water. *Bioresource Technology, 118*, 536–544. https://doi.org/10.1016/j.biortech.2012.05.042.

Arafat, H. A., Franz, M., & Pinto, N. G. (1999). Effect of salt on the mechanism of adsorption of aromatics on activated carbon. *Langmuir : the ACS journal of surfaces and colloids, 15*(18), 5997–6003.

Bekkouche, S., Baup, S., Bouhelassa, M., Molina-Boisseau, S., & Petrier, C. (2012). Competitive adsorption of phenol and heavy metal ions onto titanium dioxide (Dugussa P25). *Desalination and Water Treatment, 37*(1–3), 364–372.

Calace, N., Nardi, E., Petronio, B., & Pietroletti, M. (2002). Adsorption of phenols by papermill sludges. *Environmental Pollution, 118*(3), 315–319.

Cely, P., Tarquis, A. M., Paz-Ferreiro, J., Méndez, A., & Gascó, G. (2014). Factors driving the carbon mineralization priming effect in a sandy loam soil amended with different types of biochar. *Solid Earth, 5*(1), 585–594. https://doi.org/10.5194/se-5-585-2014.

Chen, B., & Chen, Z. (2009). Sorption of naphthalene and 1-naphthol by biochars of orange peels with different pyrolytic temperatures. *Chemosphere, 76*(1), 127–133. https://doi.org/10.1016/j.chemosphere.2009.02.004.

Chen, B., Zhou, D., & Zhu, L. (2008). Transitional adsorption and partition of nonpolar and polar aromatic contaminants by biochars of pine needles with different pyrolytic temperatures. *Environmental Science & Technology, 42*(14), 5137–5143.

Chen, Z., Chen, B., Zhou, D., & Chen, W. (2012). Bisolute sorption and thermodynamic behavior of organic pollutants to biomass-derived biochars at two pyrolytic temperatures. *Environmental Science & Technology, 46*(22), 12476–12483. https://doi.org/10.1021/es303351e.

Cui, Y., Liu, X. Y., Chung, T. S., Weber, M., Staudt, C., & Maletzko, C. (2016). Removal of organic micro-pollutants (phenol, aniline and nitrobenzene) via forward osmosis (FO) process: evaluation of FO as an alternative method to reverse osmosis (RO). *Water Research, 91*, 104–114. https://doi.org/10.1016/j.watres.2016.01.001.

Demirbas, A. (2004). Effects of temperature and particle size on bio-char yield from pyrolysis of agricultural residues. *Journal of Analytical and Applied Pyrolysis, 72*(2), 243–248. https://doi.org/10.1016/j.jaap.2004.07.003.

Dong, X., Ma, L. Q., Zhu, Y., Li, Y., & Gu, B. (2013). Mechanistic investigation of mercury sorption by Brazilian pepper biochars of different pyrolytic temperatures based on X-ray photoelectron spectroscopy and flow calorimetry. *Environmental Science & Technology, 47*(21), 12156–12164. https://doi.org/10.1021/es4017816.

Garcia-Segura, S., Ocon, J. D., & Chong, M. N. (2018). Electrochemical oxidation remediation of real wastewater effluents — a review. *Process Safety and Environmental Protection, 113*, 48–67. https://doi.org/10.1016/j.psep.2017.09.014.

Gupta, S., Kua, H. W., & Koh, H. J. (2018). Application of biochar from food and wood waste as green admixture for cement mortar. *The Science of the Total Environment, 619-620*, 419–435. https://doi.org/10.1016/j.scitotenv.2017.11.044.

Hamdaoui, O., & Naffrechoux, E. (2007). Modeling of adsorption isotherms of phenol and chlorophenols onto granular activated carbon Part I. Two-parameter models and equations allowing determination of thermodynamic parameters. *Journal of hazardous materials, 147*(1–2), 381–394. https://doi.org/10.1016/j.jhazmat.2007.01.021.

Han, Y., Boateng, A. A., Qi, P. X., Lima, I. M., & Chang, J. (2013). Heavy metal and phenol adsorptive properties of biochars from pyrolyzed switchgrass and woody biomass in correlation with surface properties. *Journal of Environmental Management, 118*, 196–204. https://doi.org/10.1016/j.jenvman.2013.01.001.

Honfi, K., Tálos, K., Kőnig-Péter, A., Kilár, F., & Pernyeszi, T. (2016). Copper (II) and phenol adsorption by cell surface treated Candida tropicalis cells in aqueous suspension. *Water, Air, & Soil Pollution, 227*(2), 61.

Idrees, M., Batool, S., Kalsoom, T., Yasmeen, S., Kalsoom, A., Raina, S., et al. (2018). Animal manure-derived biochars produced via fast pyrolysis for the removal of divalent copper from aqueous media. *Journal of Environmental Management, 213*, 109–118. https://doi.org/10.1016/j.jenvman.2018.02.003.

Jain, A. K., Gupta, V. K., Jain, S., & Suhas. (2004). Removal of chlorophenols using industrial wastes. *Environmental Science & Technology, 38*(4), 1195–1200.

Javed, H., Luong, D. X., Lee, C.-G., Zhang, D., Tour, J. M., & Alvarez, P. J. J. (2018). Efficient removal of bisphenol-A by ultra-high surface area porous activated carbon derived from asphalt. *Carbon, 140*, 441–448. https://doi.org/10.1016/j.carbon.2018.08.038.

Julcour Lebigue, C., Andriantsiferana, C., N'Guessan, K., Ayral, C., Mohamed, E., Wilhelm, A. M., et al. (2010). Application of sludge-based carbonaceous materials in a hybrid water treatment process based on adsorption and catalytic wet air oxidation. *Journal of Environmental Management, 91*(12), 2432–2439. https://doi.org/10.1016/j.jenvman.2010.06.008.

Jung, C., Park, J., Lim, K. H., Park, S., Heo, J., Her, N., et al. (2013). Adsorption of selected endocrine disrupting compounds and pharmaceuticals on activated biochars. *Journal of Hazardous Materials, 263*(Pt 2), 702–710. https://doi.org/10.1016/j.jhazmat.2013.10.033.

Kalderis, D., Kayan, B., Akay, S., Kulaksız, E., & Gözmen, B. (2017). Adsorption of 2,4-dichlorophenol on paper sludge/wheat husk biochar: process optimization and comparison with biochars prepared from wood chips, sewage sludge and hog fuel/demolition waste. *Journal of Environmental Chemical Engineering, 5*(3), 2222–2231. https://doi.org/10.1016/j.jece.2017.04.039.

Karakoyun, N., Kubilay, S., Aktas, N., Turhan, O., Kasimoglu, M., Yilmaz, S., et al. (2011). Hydrogel–Biochar composites for effective organic contaminant removal from aqueous media. *Desalination, 280*(1–3), 319–325. https://doi.org/10.1016/j.desal.2011.07.014.

Kim, M. H., & Kim, J. W. (2010). Comparison through a LCA evaluation analysis of food waste disposal options from the perspective of global warming and resource recovery. *The Science of the Total Environment, 408*(19), 3998–4006. https://doi.org/10.1016/j.scitotenv.2010.04.049.

Kim, T. Y., Cho, S. Y., & Kim, S. J. (2010). Adsorption equilibrium and kinetics of copper ions and phenol onto modified adsorbents. *Adsorption, 17*(1), 135–143. https://doi.org/10.1007/s10450-010-9306-2.

Kim, Y. S., Jang, J. Y., Park, S. J., & Um, B. H. (2018a). Dilute sulfuric acid fractionation of Korean food waste for ethanol and lactic acid production by yeast. *Waste Management, 74*, 231–240. https://doi.org/10.1016/j.wasman.2018.01.012.

Kim, H. B., Kim, S. H., Jeon, E. K., Kim, D. H., Tsang, D. C. W., Alessi, D. S., et al. (2018b). Effect of dissolved organic carbon from sludge, rice straw and spent coffee ground biochar on the mobility of arsenic in soil. *The Science of the Total Environment, 636*, 1241–1248. https://doi.org/10.1016/j.scitotenv.2018.04.406.

Lazo-Cannata, J. C., Nieto-Márquez, A., Jacoby, A., Paredes-Doig, A. L., Romero, A., Sun-Kou, M. R., et al. (2011). Adsorption of phenol and nitrophenols by carbon nanospheres: effect of pH and ionic strength. *Separation and Purification Technology, 80*(2), 217–224. https://doi.org/10.1016/j.seppur.2011.04.029.

Lee, D. H., Behera, S. K., Kim, J. W., & Park, H. S. (2009). Methane production potential of leachate generated from Korean food waste recycling facilities: a lab-scale study. *Waste Management, 29*(2), 876–882. https://doi.org/10.1016/j.wasman.2008.06.033.

Lee, C.-G., Park, J.-A., Choi, J.-W., Ko, S.-O., & Lee, S.-H. (2016). Removal and recovery of Cr(VI) from industrial plating wastewater using fibrous anion exchanger. *Water, Air, & Soil Pollution, 227*(8). https://doi.org/10.1007/s11270-016-2992-y.

Lee, C. G., Javed, H., Zhang, D., Kim, J. H., Westerhoff, P., Li, Q., et al. (2018). Porous electrospun fibers embedding TiO2 for adsorption and photocatalytic degradation of water pollutants. *Environmental Science & Technology, 52*(7), 4285–4293. https://doi.org/10.1021/acs.est.7b06508.

Li, H., Mahyoub, S. A. A., Liao, W., Xia, S., Zhao, H., Guo, M., et al. (2017). Effect of pyrolysis temperature on characteristics and aromatic contaminants adsorption behavior of magnetic biochar derived from pyrolysis oil distillation residue. *Bioresource Technology, 223*, 20–26. https://doi.org/10.1016/j.biortech.2016.10.033.

Lin, S. H., & Juang, R. S. (2009). Adsorption of phenol and its derivatives from water using synthetic resins and low-cost natural adsorbents: a review. *Journal of Environmental Management, 90*(3), 1336–1349. https://doi.org/10.1016/j.jenvman.2008.09.003.

Liu, Z., & Zhang, F.-S. (2011). Removal of copper (II) and phenol from aqueous solution using porous carbons derived from hydrothermal chars. *Desalination, 267*(1), 101–106. https://doi.org/10.1016/j.desal.2010.09.013.

Liu, Q.-S., Zheng, T., Wang, P., Jiang, J.-P., & Li, N. (2010). Adsorption isotherm, kinetic and mechanism studies of some substituted phenols on activated carbon fibers. *Chemical Engineering Journal, 157*(2–3), 348–356. https://doi.org/10.1016/j.cej.2009.11.013.

Liu, Y., Chen, J., Chen, M., Zhang, B., Wu, D., & Cheng, Q. (2015). Adsorption characteristics and mechanism of sewage sludge-derived adsorbent for removing sulfonated methyl phenol resin in wastewater. *RSC Advances, 5*(93), 76160–76169.

Mahvi, A., Maleki, A., & Eslami, A. (2004). *Potential of rice husk and rice husk ash for phenol removal in aqueous systems*.

MOE, Ministry of Environment Korea (2017). *Food waste reduction and resource reclamation*.

Mukherjee, S., Kumar, S., Misra, A. K., & Fan, M. (2007). Removal of phenols from water environment by activated carbon, bagasse ash and wood charcoal. *Chemical Engineering Journal, 129*(1–3), 133–142. https://doi.org/10.1016/j.cej.2006.10.030.

Ou, Y.-H., Chang, Y.-J., Lin, F.-Y., Chang, M., Yang, C.-Y., & Shih, Y.-H. (2016). Competitive sorption of bisphenol A and phenol in soils and the contribution of black carbon. *Ecological Engineering, 92*, 270–276. https://doi.org/10.1016/j.ecoleng.2016.04.006.

Papaevangelou, V. A., Gikas, G. D., Tsihrintzis, V. A., Antonopoulou, M., & Konstantinou, I. K. (2016). Removal of endocrine disrupting chemicals in HSF and VF pilot-scale constructed wetlands. *Chemical Engineering Journal, 294*, 146–156. https://doi.org/10.1016/j.cej.2016.02.103.

Peng, P., Lang, Y.-H., & Wang, X.-M. (2016). Adsorption behavior and mechanism of pentachlorophenol on reed biochars: pH effect, pyrolysis temperature, hydrochloric acid treatment and isotherms. *Ecological Engineering, 90*, 225–233. https://doi.org/10.1016/j.ecoleng.2016.01.039.

Polat, H., Molva, M., & Polat, M. (2006). Capacity and mechanism of phenol adsorption on lignite. *International Journal of Mineral Processing, 79*(4), 264–273.

Rago, Y. P., Surroop, D., & Mohee, R. (2018). Assessing the potential of biofuel (biochar) production from food wastes through thermal treatment. *Bioresource Technology, 248*(Pt A), 258–264. https://doi.org/10.1016/j.biortech.2017.06.108.

Regmi, P., Garcia Moscoso, J. L., Kumar, S., Cao, X., Mao, J., & Schafran, G. (2012). Removal of copper and cadmium from aqueous solution using switchgrass biochar produced via hydrothermal carbonization process. *Journal of Environmental Management, 109*, 61–69. https://doi.org/10.1016/j.jenvman.2012.04.047.

Shin, W.-S. (2017). Adsorption characteristics of phenol and heavy metals on biochar from Hizikia fusiformis. *Environmental Earth Sciences, 76*(22). https://doi.org/10.1007/s12665-017-7125-4.

Substances, A. F. T., & Registry, D. (1998). *Toxicological profile for phenol (update)*. GA: Public Health Service, US Department of Health and Human Services Atlanta.

Varghese, S., Vinod, V., & Anirudhan, T. (2004). *Kinetic and equilibrium characterization of phenols adsorption onto a novel activated carbon in water treatment*.

Víctor-Ortega, M. D., Ochando-Pulido, J. M., & Martínez-Férez, A. (2016). Phenols removal from industrial effluents through novel polymeric resins: kinetics and equilibrium studies. *Separation and Purification Technology, 160*, 136–144. https://doi.org/10.1016/j.seppur.2016.01.023.

Vikrant, K., Kim, K. H., Ok, Y. S., Tsang, D. C. W., Tsang, Y. F., Giri, B. S., et al. (2018). Engineered/designer biochar for the removal of phosphate in water and wastewater. *The Science of the Total Environment, 616-617*, 1242–1260. https://doi.org/10.1016/j.scitotenv.2017.10.193.

Villegas, L. G. C., Mashhadi, N., Chen, M., Mukherjee, D., Taylor, K. E., & Biswas, N. (2016). A short review of techniques for phenol removal from wastewater. *Current Pollution Reports, 2*(3), 157–167. https://doi.org/10.1007/s40726-016-0035-3.

Vithanage, M., Mayakaduwa, S. S., Herath, I., Ok, Y. S., & Mohan, D. (2016). Kinetics, thermodynamics and mechanistic studies of carbofuran removal using biochars from tea waste and rice husks. *Chemosphere, 150*, 781–789. https://doi.org/10.1016/j.chemosphere.2015.11.002.

Xie, J., Meng, W., Wu, D., Zhang, Z., & Kong, H. (2012). Removal of organic pollutants by surfactant modified zeolite: comparison between ionizable phenolic compounds and non-ionizable organic compounds. *Journal of Hazardous Materials, 231-232*, 57–63. https://doi.org/10.1016/j.jhazmat.2012.06.035.

Yang, X., Igalavithana, A. D., Oh, S. E., Nam, H., Zhang, M., Wang, C. H., et al. (2018). Characterization of bioenergy biochar and its utilization for metal/metalloid immobilization in contaminated soil. *The Science of the Total Environment, 640-641*, 704–713. https://doi.org/10.1016/j.scitotenv.2018.05.298.

Zagklis, D. P., Vavouraki, A. I., Kornaros, M. E., & Paraskeva, C. A. (2015). Purification of olive mill wastewater phenols through membrane filtration and resin adsorption/desorption. *Journal of Hazardous Materials, 285*, 69–76. https://doi.org/10.1016/j.jhazmat.2014.11.038.

Zhang, D., Lee, C., Javed, H., Yu, P., Kim, J. H., & Alvarez, P. J. J. (2018). Easily-recoverable, micron-sized TiO2 hierarchical spheres decorated with cyclodextrin for enhanced photocatalytic degradation of organic micropollutants. *Environmental Science & Technology*. https://doi.org/10.1021/acs.est.8b04301.

Zheng, H., Guo, W., Li, S., Chen, Y., Wu, Q., Feng, X., et al. (2017). Adsorption of p-nitrophenols (PNP) on microalgal biochar: analysis of high adsorption capacity and mechanism. *Bioresource Technology, 244*(Pt 2), 1456–1464. https://doi.org/10.1016/j.biortech.2017.05.025.

Zhou, X., Zhou, J., Liu, Y., Wang, Y., Ren, J., & Ling, B. (2018). Preparation of magnetic biochar derived from cyclosorus interruptus for the removal of phenolic compounds: characterization and mechanism. *Separation Science and Technology, 53*(9), 1307–1318. https://doi.org/10.1080/01496395.2018.1444056.